Available online at www.sciencedirect.com
ScienceDirect
Ceramics International 34 (2008) 971–977
CERAMICS INTERNATIONAL
www.elsevier.com/locate/ceramint

Si field emitter arrays coated with thin ferroelectric films

X.F. Chen [a,*], W. Zhu [b], H. Lu [b], J.S. Pan [c], H.J. Bian [b], O.K. Tan [b], C.Q. Sun [b]

[a] Electronic Materials Research Laboratory, Key Laboratory of the Ministry of Education, Xi'an Jiaotong University, Xi'an 710049, China
[b] Microelectronics Centre, School of Electrical and Electronic Engineering, Nanyang Technological University, Nanyang Avenue, Singapore 639798
[c] Institute of Materials Research & Engineering, 3 Research Link, Singapore 117602

Available online 2 October 2007

Abstract

This paper demonstrates novel approach on Si field emitter arrays (FEAs) coated with thin ferroelectric films for vacuum microelectronic applications, which exhibit enhanced electron emission behaviors. The films were deposited using sol–gel and sputtering process, respectively. In sol–gel approach, the emission behavior is highly correlated to the crystallinity of (Ba,Sr)TiO_3 (BST) layer. The interfacial reaction between Si and BST film would deteriorate the crystallinity of the films, and in turn impede the electron emission from silicon tips. The film thickness and the dopants also affect the emission behaviors significantly. In sputtering process, the nitrogen-incorporated $SrTiO_3$ (STO) films are deposited with eliminated interfacial due to relatively lower processing temperature. The enhanced emission characteristics are highly correlated with nitrogen-incorporation and film thickness. These encouraging results have offered great promise for the application of ferroelectric films in field emission devices.

Keywords: Field emission; Ferroelectric thin films

1. Introduction

Field emission (FE) is usually based on the physical phenomenon of quantum tunneling, in which electrons are injected from the surface of materials into vacuum under the applied electric field. Compared to thermionic cathode vacuum tubes, the field emission devices could offer some unique advantages, such as compact size, modest power consumption and possibility to integrate with solid-state electronics. They have a number of important applications both in military and domestic industries, including flat panel displays, microcolumns for electron beam parallel writing, various types of vacuum microelectronic devices, RF devices, vacuum sensors and space instruments [1]. To date, a variety of field emission cold cathode materials have been developed, including materials for microfabricated field emitter arrays, diamond and related films, quasi one-dimensional nanomaterials like carbon nanotubes and ferroelectric materials. Recently, the enhanced electron emission behavior from the $Ba_{0.66}Sr_{0.33}TiO_3$ (BST)-coated silicon tip arrays was discovered by Kang [2,3] and Zhu [4]. BST is a well-known material in ferroelectric family. However, the emission current from BST film surface is different from the so-called ferroelectric electron emission (FEE). It is known that FEE is an unconventional electron emission effect [5,6] and generated by a deviation of spontaneous polarization from the equilibrium state under pyroelectric, piezoelectric effects, or polarization reversal. In contrast, the emission current from BST thin films demonstrates a steady state current and is much similar to the classic types of electron emission from the solids. The emission behavior is found to be highly correlated with their structure [2,3] and stoichiometric composition [4]. In this paper, we summarize our recent advances on the enhanced field emission of BST films coated on microfabricated Si field emitter arrays (FEAs) via sol–gel and sputtering process. Moreover, a series of structural studies for understanding the corresponding mechanism is given also.

2. Field emission from BST thin films

Firstly, Si FEAs were fabricated using conventional microfabrication techniques, like photolithographic patterning, silicon anisotropic etching, oxidation for tip sharpening, and

* Corresponding author. Tel.: +86 29 82668584; fax: +86 29 82668794.
E-mail address: exfchen@mail.xjtu.edu.cn (X.F. Chen).

0272-8842/$34.00
doi:10.1016/j.ceramint.2007.09.084

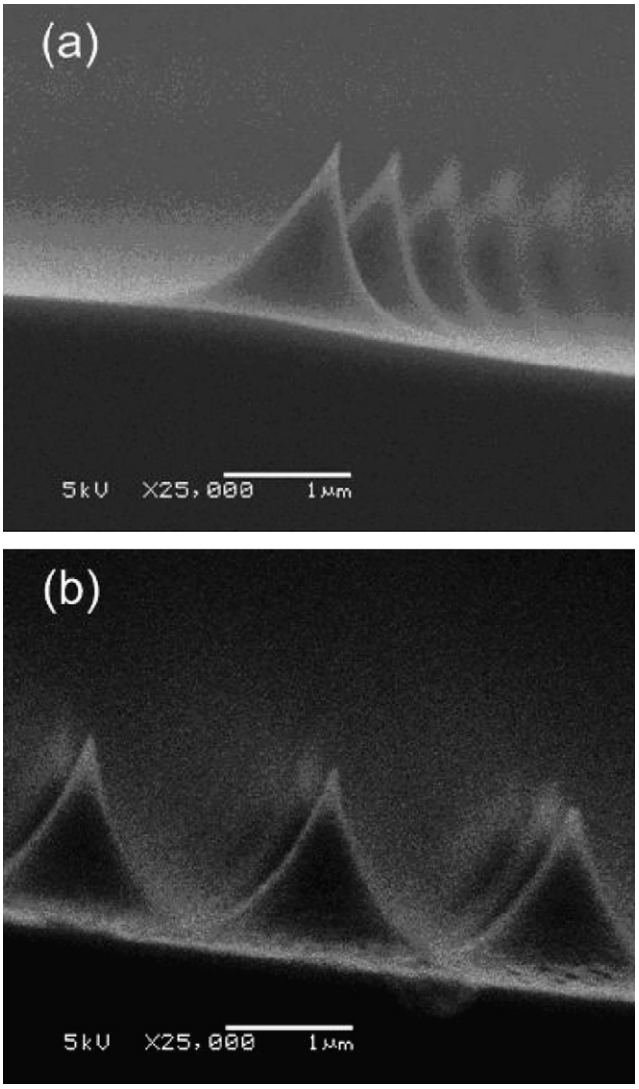

Fig. 1. SEM pictures (SEM) of (a) uncoated Si FEAs and (b) that coated with 30-nm-thick BST films.

buffered oxide etching. The *n*-type Si wafers with the resistivity of 2–5 Ω cm were used as FEA substrate and the tip height was controlled around 1 μm. Then, the BST thin films were coated on fabricated Si FEAs using sol–gel process detailed elsewhere [7]. Fig. 1 demonstrates the SEM pictures of the Si FEAs before (a) and after (b) BST coating. Field emission measurement was carried out in custom-made vacuum chamber with the vacuum up to 10^{-7} mbar, as shown in Fig. 2. A stainless steel base was used to make electrical contact to the Si FEAs, and an ITO glass with a sheet resistance of 10 Ω/□ was placed 50 μm above the cathode as an anode via a Teflon spacer. In the opened Teflon hole, around 10^4 tips were exposed for electron emission measurement. The threshold field was defined using an arbitrary criterion as the voltage required to produce a current of 1 pA per tip, corresponding to SNR over 1000.

It is observed that the field emission phenomenon of BST-coated Si FEAs is much sensitive to annealing temperature and film thickness as illustrated in Fig. 3 [7,8]. Such sensitivity is believed to originate from the structural feature of BST films. It is shown that the threshold electric field could be largely lowered from 36 V/μm for the bare Si FEAs to 19 V/μm for that with a 30-nm-thick BST coating annealed at 700 °C. The films annealed at 600 °C are amorphous in general with threshold field about 28.5 V/μm, and there is no encouraging improvement found due to its electric insulating nature. However, further increasing annealing temperature above 750 °C does not lead to further improvement in electron emission behavior. Instead, the interfacial reaction takes place at the BST/Si interface. The occurred interfacial reaction results in poorer crystallinity of BST layer, which might respond for the degradation of the electron emission behavior. Moreover, the thickness of BST layer also impacts on the development of perovskite grains in the films. The 15-nm-thick film on Si wafer is general in amorphous and the perovskite grains can be found in 30-nm-thick films. The measurement results indicate that the optimized thickness to achieve the lowest threshold field is around 30 nm. Moreover, BST-coated Si FEAs also demonstrated improved stability for electron emission. Fig. 4 compares the emission current stability of three

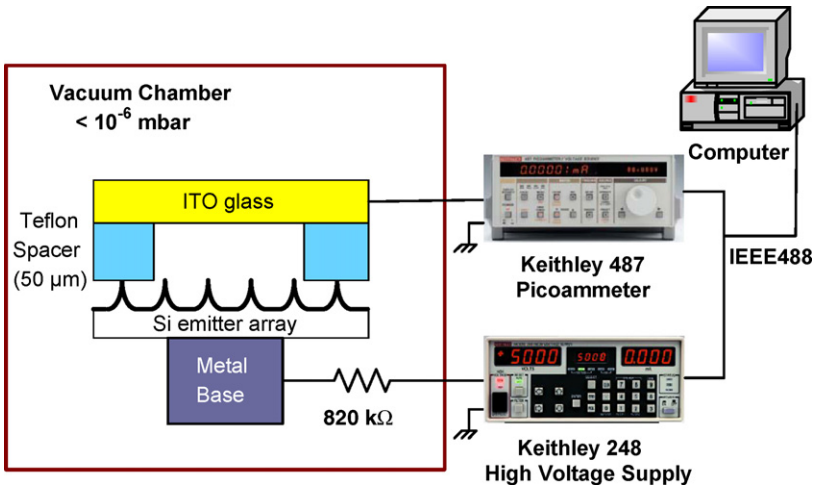

Fig. 2. Schematic diagram of the electron field emission characterization set up.

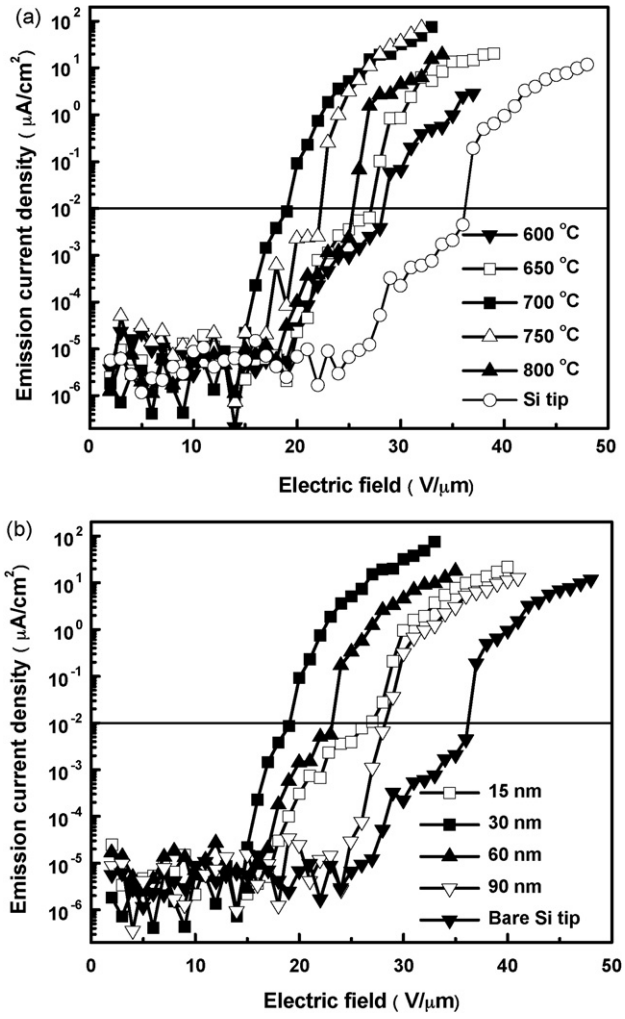

Fig. 3. (a) Effect of annealing temperature on field emission of Si FEAs coated with 30-nm-thick BST thin films and (b) thickness effects on that of BST-coated Si FEAs annealed at 700 °C.

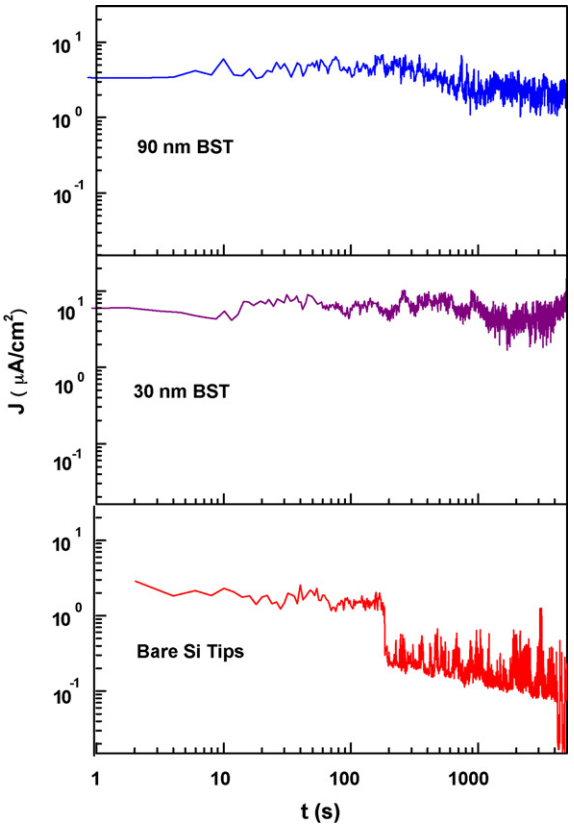

Fig. 4. The emission current stability of uncoated Si FEAs and BST-coated Si FEAs with thickness of 30 nm and 90 nm respectively, annealed at 700 °C.

kinds of Si FEAs, namely bare Si FEAs and that coated with 30-nm-thick and 90-nm-thick BST film respectively, annealed at 700 °C.

Such enhanced field emission characteristic originates from the lowering of effective work-function of Si tips after BST coating. The corresponding effective work-function can be estimated according to Flowler–Nordiem (F–N) relationship as detailed elsewhere

$$I = aV^2 \exp\left(-\frac{b\phi^{3/2}}{V}\right) \quad (1)$$

where a and b are constant, I is the emission current, and ϕ is the work-function of the emitting surface. Assuming the tunneling barrier height of Si to be 4.3 eV, corresponding to the work-function of n-type silicon with 2 Ω cm resistivity we used, the effective work-function of BST-coated tips can be deduced from the ratio of F–N slope of BST-coated silicon tip to that of uncoated tip, as listed in Table 1. The Si FEAs coated with 30-nm-thick BST films annealed at 700 °C demonstrated the lowest effective work-function of 2.3 eV.

Table 1
The threshold field, FNSL parameters, and the effective work-function of BST-coated Si FEAs as a function of annealing temperature and film thickness

Annealing temperature (°C)	Thickness of BST (nm)	Threshold field (V/μm)	$FNSL_{BST}/FNSL_{Si}$	ϕ_{BST} (eV)
600	30	28.5	0.93	4.1
650	30	27	0.69	3.4
700	15	27	0.57	2.9
700	30	19	0.40	2.3
700	60	23	0.46	2.5
700	90	28	0.65	3.3
750	30	22.5	0.48	2.6
800	30	25.2	0.50	2.7

Up to now, the mechanism for such enhanced field emission behaviors is not well-understood yet. For general understanding, the field emission process of BST-coated Si FEAs would experience three major steps, including supply electrons to BST film, electron transport to surface, and electron emission into vacuum. Therefore, some material issues including the interfacial structure between BST film and Si tip, microstructural features in BST film, and energy diagram of emitter surface would affect electron transport in different steps accordingly. For examples, the structure development of the films would be affected by their thickness and annealing temperature. In high-resolution electron microscopy (HREM) observation, the 15-nm-thick BST film annealed at 700 °C is amorphous in general. With thickness increasing, there is a two-layered structure observed, an amorphous layer near Si wafer and a polycrystalline layer at the top surface. Fig. 5 illustrates a typical cross-sectional HREM image of 30-nm-thick BST films annealed at 700 °C. Moreover, the clear interface contrast can be observed at BST/Si interface, which is attributed to the formation of silicon oxide interfacial layer during sol–gel process. Second ion mass spectroscopy (SIMS) analysis was also performed to clarify the interface structure. It is shown that there is a mixture region with Ba, Sr, Ti, Si and O presented at BST/Si interface. The mixture layer originates from the solid-state reaction between BST and Si during the annealing process, corresponding to (Ba,Sr)$Ti_xSi_yO_z$. With annealing temperature increasing, the reaction is promoted showing the broadened

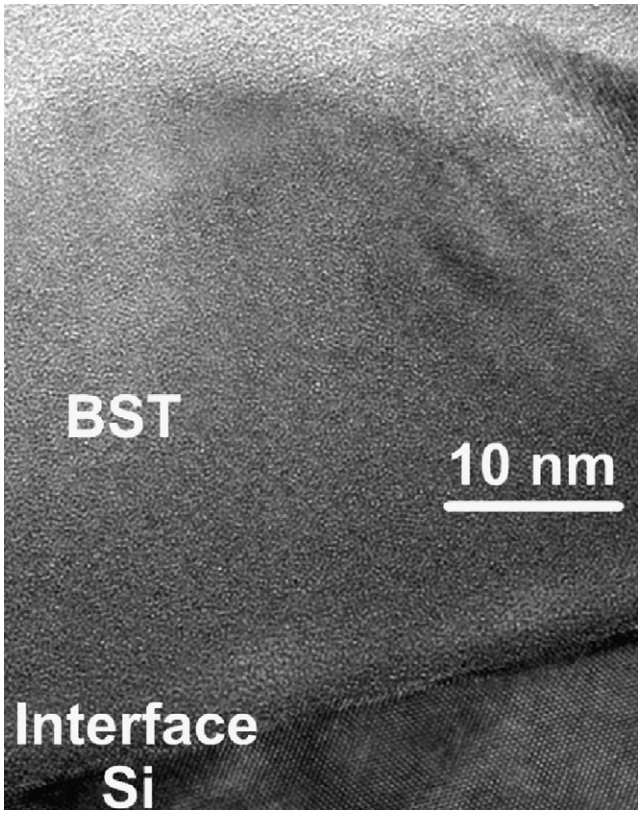

Fig. 5. Cross-sectional HREM images of sol–gel derived 30-nm-thick BST thin films annealed at 700 °C.

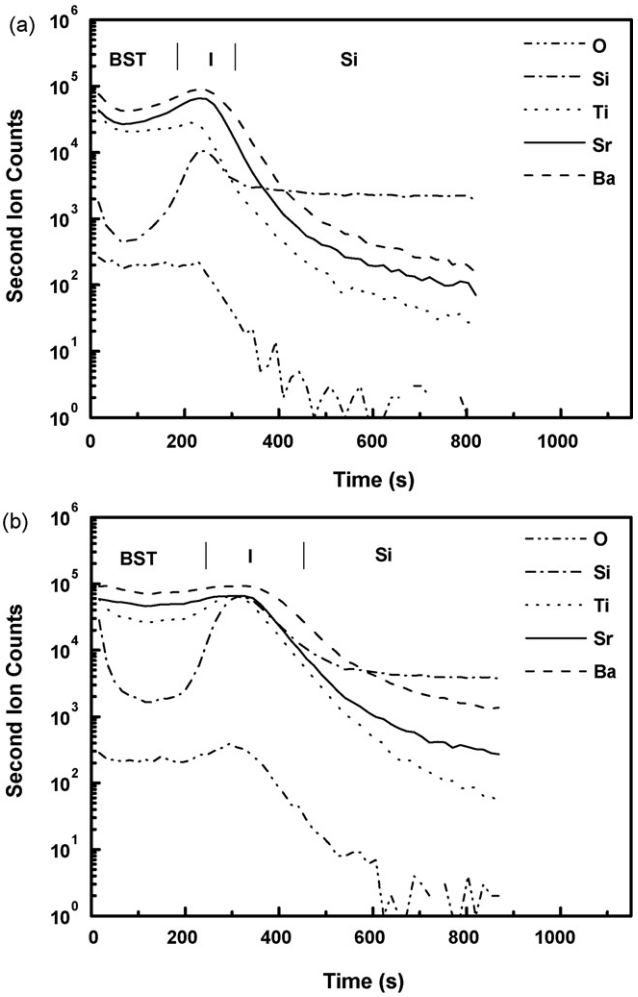

Fig. 6. SIMS depth profiles for sol–gel BST thin film annealed at (a) 700 °C and (b) 800 °C for 1 h.

overlapping region of Si, Ba, Sr, Ti and O profiles, as illustrated in Fig. 6.

Moreover, the surface construction would affect the field emission behaviors also. X-ray photoelectron spectroscopy (XPS) study on the Ba $3d_{5/2}$ core level spectra of BST films gives a clear picture on the emitter surface structure [9]. It is know that the Ba $3d_{5/2}$ spectrum is composed of two peaks with the lower binding energy at 779.1 eV and the high binding energy at 780.5 eV, corresponding to the coordinated $Ba_{(1)}$ and uncoordinated $Ba_{(2)}$, respectively. As shown in Fig. 7(a), the coordinated Ba peak could only be observed in the films annealed at 700 and 750 °C, indicating the formation of perovskite grains on the surface. Similarly, only the uncoordinated Ba could be found in 15-nm-thick BST film, indicating amorphous state at the surface. The coordinated Ba could be observed in the films with thickness above 30 nm and its content increase substantially with thickness increasing as shown in Fig. 7(b).

In perovskite structure, the corner-shared TiO_6 octahedra dominate the main electronic properties of BST. In a simplified ionic model, it would lead to a completely full O 2p valence band and an empty Ti 3d conduction band for BST. Therefore,

Table 2
Summary of measured bandgap energy, and shift value of the Fermi level ΔE_F, valence-band maximum (VBM) (ΔE_{VBM}), conduction-band minimum (CBM) (ΔE_{CBM}) of BST thin films annealed different temperatures

Annealing temperature (°C)	Bandgap (eV)	ΔE_F (eV)	ΔE_{VBM} (eV)	ΔE_{CBM} (eV)
600	4.16	–	–	–
650	4.09	0.13	−0.06	−0.01
700	3.86	0.24	−0.13	−0.17
750	3.99	0.49	−0.25	0.08
800	4.02	0.29	−0.26	0.12

surface structure change would accompany the modification of energy diagram of BST film surface, which can be estimated using XPS. Maintaining the constant thickness, the influence of annealing temperature on energy diagram of BST films was investigated as detailed elsewhere [9]. Table 2 lists the shifts of energy diagram of the films annealed at different temperatures. Referred to amorphous BST films annealed at 600 °C, the polycrystalline BST film annealed at 700 °C exhibits narrowed bandgap, upwards-moved Fermi level and downwards-moved conduction-band minimum (CBM), which are believed to contribute to the enhanced field emission of BST-coated Si FEAs. Further increasing annealing temperature would result in the interfacial reaction and degraded crystallinity in the films, which might deteriorate the electron emission accordingly. However, it is difficult to estimate the thickness effect on Fermi level shift of the films because the binding energy shift of Ti 2p is also affected by the band bending in the films owing to space-charge distribution.

3. Field emission from La-doped BST thin films

As discussed above, it is possible to improve electron emission performance further by introducing transition metal dopant to achieve *n*-type conduction in BST films. La^{3+} or Nb^{5+} are the typical transition metal dopant used to substitute Ba^{2+}(Sr^{2+}) or Ti^{4+} sites in BST films, respectively. In particular, La^{3+} substitution of Ba^{2+}/Sr^{2+} sites in the lattice would introduce electrons into the conduction band of BST [10]. It is reported that metallic $Sr_{1-x}La_xTiO_3$ solid-solution could be achieved with La composition range between 0.1 and 1, whereas the concentration below 0.1 would result in carrier localization effect due to poor shielding of the impurity (La^{3+}) potential by low carrier density [11].

Hence, our study was extended by applying La-doped BST (BSLT) film on Si FEAs for field emission applications. It is revealed that with La introduction, the interfacial reaction between Si and BSLT film could be eliminated, and in turn the annealing temperature was increased up to 750 °C to achieve better crystallinity. As shown in Fig. 8, the BSLT coating with moderate La concentration ($x = 0.25$) shows the improvement of field emission of Si tip arrays with respect to the BST ($x = 0$) coating. The threshold field can be lowered further from 19 V/μm for BST ($x = 0$) film to about 15 V/μm for BSLT ($x = 0.25$) film. However, there is no obvious improvement of field emission observed while the coated BSLT films were doped

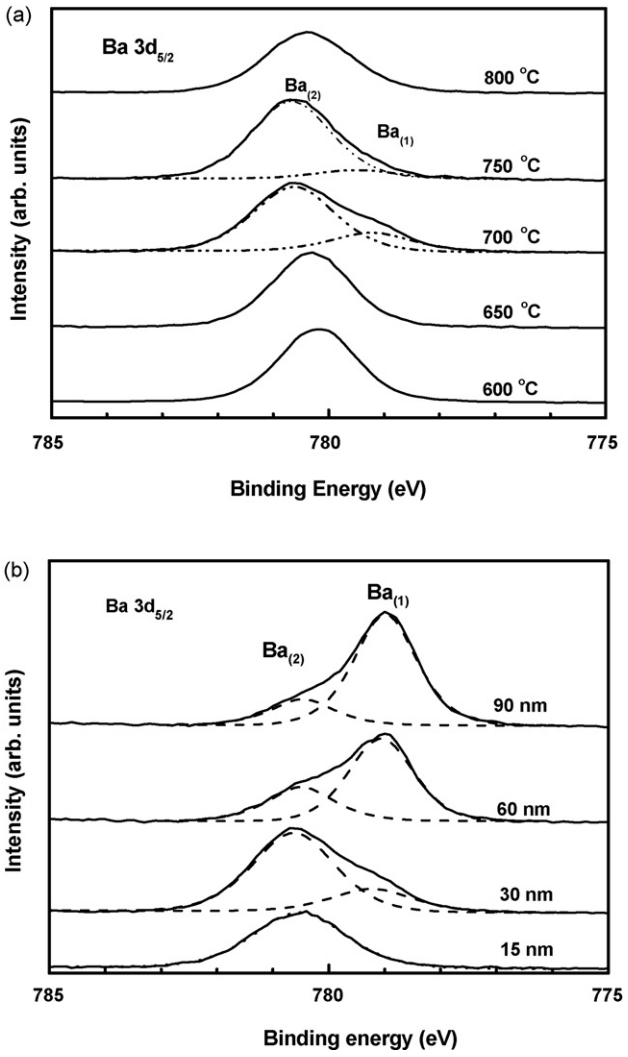

Fig. 7. XPS Ba $3d_{5/2}$ core level spectra of (a) 30-nm-thick BST thin films annealed at different temperatures and (b) the films annealed at 700 °C with different thicknesses.

with extremely lower ($x = 0.1$) and higher ($x \geq 0.75$) La concentration.

It is believed that such improvement might relate to the structural development in BSLT films, which is highly depended on the doped La level. The films are perovskite-phase dominated at La doping level within 0.5 and pyrochlore-phase dominated at high La content over 0.75, respectively. Both HREM observation and Ba $3d_{5/2}$ spectra study reveal that perovskite BSLT film with La content around 0.25 demonstrates well-developed perovskite structure in the surface region and the suppressed interfacial reaction.

The La doping would alter the electronic structure in BST film, and affect their emission properties accordingly. Generally, La^{3+} cations, substituting Ba^{2+}/Sr^{2+} sites in the lattice, act as a donor-type dopant in the film. It is revealed in XPS study that the Fermi level shifts downward about −0.17 eV for the film with low La content ($x = 0.1$), referring to that of the undoped BST film. It is known that the low La doping level would lead to the remarkable decrease of oxygen vacancy. With

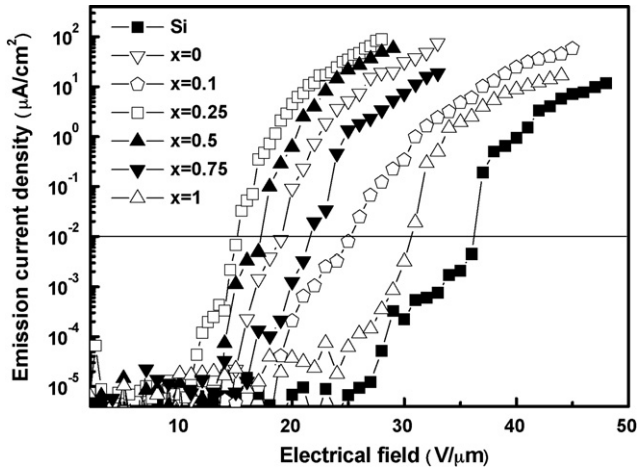

Fig. 8. Field emission of Si FEAs coated with 30-nm-thick sol–gel BSLT thin films annealed at 750 °C.

moderate La doping of $x = 0.25$, the Fermi level demonstrates upward shift of 0.25 eV with respect to that of undoped BST film, and result in a lower of work-function accordingly. However, further increasing La concentration over 0.5 would result in downward shift of the Fermi level in BSLT films.

4. Field emission from sputtered BST thin films with nitrogen-incorporation

As an alternative way, RF magnetron sputtering is regarded as one of effective ways to eliminate the interface reaction between BST and Si tips and to provide better conformal coverage on Si tips as well. In sputtering process, the microstructure evolution and stoichiometric composition of the films are much sensitive to the sputtering parameters. In particular, the sputtering gas is one of important parameters to affect the stoichiometric composition in the films. In experimental, three kinds of sputtering gases were used to verify the impact of induced electronic defects on the field emission behaviors of $SrTiO_3$ (STO) films. The gases used included pure Ar, mixture of Ar–20%O_2, and mixture of Ar–50%N_2, respectively. It is known that the film deposited in pure Ar ambient was usually oxygen-deficient, and oxygen was introduced to compensate the oxygen loss in the films. It is interesting that deposition in mixed gas of Ar and N_2 would lead to nitrogen-incorporation into STO films [12]. Substitution of a non-metallic atom such as nitrogen for oxygen in $SrTiO_3$ (STO) [13] and in TiO_2 [14] has proven to lead to narrowed bandgap because its p states contribute to the bandgap narrowing by mixing with O 2p states, which might benefit the enhanced field emission properties also. Fig. 9 illustrates the field emission characteristics of above-mentioned films on Si FEAs with thickness of 12 nm. The N-STO and O-STO denote to the films deposited in Ar–50%N_2 and Ar–20%O_2, respectively. It is obvious that nitrogen-incorporation could enhance the field emission of $SrTiO_3$ coated silicon tip by lowering the threshold field to 17 V/μm. In experimental, the nitrogen-incorporation in STO films has been confirmed using Fourier transform infrared spectroscopy (FTIR), Auger electron spectroscopy (AES) and XPS, respectively. The preliminary results show that the field emission properties of STO coated Si FEAs are also depended on the nitrogen content in the films [12]. However, the detailed state of nitrogen-incorporated in STO films has not been understood yet.

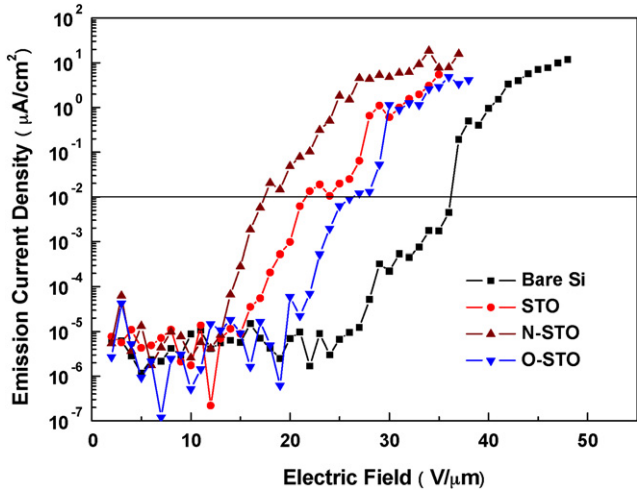

Fig. 9. Field emission of Si FEAs coated with 12-nm-thick sputtered STO thin films deposited at 600 °C.

5. Summary

Si FEAs coated with thin ferroelectric films exhibit relatively low threshold field and improved emission stability. The enhanced field emission behaviors are highly correlated to the microstructure features of coated thin ferroelectric films, the interface between Si and ferroelectric thin film, and non-stoichiometric defect and space-charge distribution in the films, which may alter their energy diagram accordingly. The detailed mechanism has not been well-understood so far. But the upwards shift of Fermi level in the films could give a reasonable explanation on such enhancement. These encouraging results would offer great promise for the application of ferroelectric films in field emission devices.

References

[1] D. Temple, Recent progress in field emitter array development for high performance applications, Mater. Sci. Eng. R24 (1999) 185–239.
[2] W.P. Kang, A. Wisitsora-at, J.L. Davidson, O.K. Tan, W. Zhu, Q. Li, J.F. Xu, Electron emission from silicon tips coated with sol–gel $Ba_{0.67}Sr_{0.33}TiO_3$ ferroelectric thin film, J. Vac. Sci. Technol. B 19 (2001) 1073–1076.
[3] W.P. Kang, A. Wisitsora-at, J.L. Davidson, O.K. Tan, W. Zhu, Q. Li, J.F. Xu, Effect of annealing temperature on the electron emission characteristics of silicon tips coated with $Ba_{0.67}Sr_{0.33}TiO_3$ thin film, J. Vac. Sci. Technol. B 21 (2003) 453–457.
[4] W. Zhu, O.K. Tan, J. Ray, M.A. Imam, X.F. Chen, Sol–gel $(Ba_{0.67}Sr_{0.33})$-Ti_xO_y thin films for flat panel display application, Integr. Ferroelectr. 49 (2002) 221–229.
[5] G. Rosenman, D. Shur, Ya.E. Krasik, A. Duaevsky, Electron emission from ferroelectrics, J. Appl. Phys. 88 (2000) 6109–6161.
[6] H. Riege, I. Boscolo, J. Handerek, U. Herleb, Features and technology of ferroelectric electron emission, J. Appl. Phys. 84 (1998) 1602–1617.

[7] X.F. Chen, H. Lu, W.G. Zhu, O.K. Tan, Enhanced field emission of silicon tips coated with sol–gel-derived $(Ba_{0.65}Sr_{0.35})TiO_3$ thin film, Surf. Coat. Technol. 198 (2005) 266–269.
[8] H. Lu, X.F. Chen, W.G. Zhu, J.S. Pan, O.K. Tan, Annealing temperature effect on field emission of silicon emitter arrays with sol–gel $(Ba_{0.65}Sr_{0.35})TiO_3$ coatings, Ferroelectrics 334 (2006) 529–537.
[9] H. Lu, J.S. Pan, X.F. Chen, W.G. Zhu, O.K. Tan, Influence of annealing temperature on the band structure of sol–gel $Ba_{0.65}Sr_{0.35}TiO_3$ thin films on *n*-type Si(1 0 0), Appl. Phys. Lett. 88 (2006) 132907.
[10] X.G. Guo, X.S. Chen, Y.L. Sun, L.S. Sun, X.H. Zhou, W. Lu, Electronic band structure of Nb doped $SrTiO_3$ from first principle calculation, Phys. Lett. A 317 (2003) 501–506.
[11] Y. Tokura, Y. Taguchi, Y. Okada, Y. Fujishima, T. Arima, Filling dependence of electronic properties on the verge of metal-mott-insulator transition in $Sr_{1-x}La_xTiO_3$, Phys. Rev. Lett. 70 (1993) 2126–2129.
[12] X.F. Chen, H. Lu, H.J. Bian, W.G. Zhu, C.Q. Sun, O.K. Tan, Electron emission of silicon field emitter arrays coated with N-doped $SrTiO_3$ film, J. Electroceram. 16 (2006) 419–423.
[13] J. Wang, S. Yin, M. Komatsu, Q. Zhang, F. Saito, T. Sato, Preparation and characterization of nitrogen doped $SrTiO_3$ photocatalyst, Appl. Catal. B: Environ. 52 (2004) 149–156.
[14] R. Asahi, T. Morikawa, T. Ohwaki, K. Aoki, Y. Taga, Visible-light photocatalysis in nitrogen-doped titanium oxides, Science 293 (2001) 269–271.